JOURNAL OF GEOPHYSICAL RESEARCH, VOL. 114, C01002, doi:10.1029/2008JC004868, 2009

Ventilation of the Arctic Ocean: Mean ages and inventories of anthropogenic CO_2 and CFC-11

Toste Tanhua,[1] E. Peter Jones,[2] Emil Jeansson,[3,4] Sara Jutterström,[3] William M. Smethie Jr.,[5] Douglas W. R. Wallace,[1] and Leif G. Anderson[3]

Received 14 April 2008; revised 4 September 2008; accepted 29 October 2008; published 3 January 2009.

[1] The Arctic Ocean constitutes a large body of water that is still relatively poorly surveyed because of logistical difficulties, although the importance of the Arctic Ocean for global circulation and climate is widely recognized. For instance, the concentration and inventory of anthropogenic CO_2 (C_{ant}) in the Arctic Ocean are not properly known despite its relatively large volume of well-ventilated waters. In this work, we have synthesized available transient tracer measurements (e.g., CFCs and SF_6) made during more than two decades by the authors. The tracer data are used to estimate the ventilation of the Arctic Ocean, to infer deep-water pathways, and to estimate the Arctic Ocean inventory of C_{ant}. For these calculations, we used the transit time distribution (TTD) concept that makes tracer measurements collected over several decades comparable with each other. The bottom water in the Arctic Ocean has CFC values close to the detection limit, with somewhat higher values in the Eurasian Basin. The ventilation time for the intermediate water column is shorter in the Eurasian Basin (~200 years) than in the Canadian Basin (~300 years). We calculate the Arctic Ocean C_{ant} inventory range to be 2.5 to 3.3 Pg-C, normalized to 2005, i.e., ~2% of the global ocean C_{ant} inventory despite being composed of only ~1% of the global ocean volume. In a similar fashion, we use the TTD field to calculate the Arctic Ocean inventory of CFC-11 to be $26.2 \pm 2.6 \times 10^6$ moles for year 1994, which is ~5% of the global ocean CFC-11 inventory.

Citation: Tanhua, T., E. P. Jones, E. Jeansson, S. Jutterström, W. M. Smethie Jr., D. W. R. Wallace, and L. G. Anderson (2009), Ventilation of the Arctic Ocean: Mean ages and inventories of anthropogenic CO_2 and CFC-11, *J. Geophys. Res.*, *114*, C01002, doi:10.1029/2008JC004868.

1. Introduction

[2] The Arctic Ocean is by volume the dominating component of the Arctic Mediterranean Sea, which additionally includes the Nordic Seas. The Arctic Ocean is landlocked, bordered by the Pacific Ocean at the Bering Strait and by the Nordic Seas in the Fram Strait and by the Barents Sea. The Arctic Mediterranean Seas are linked to the North Atlantic via exchange over the Greenland-Scotland Ridge system, where dense overflow to the south, primarily through the Denmark Strait and the Faroe Bank Channel, is an important component of the North Atlantic Deep Water and the global thermohaline circulation. The water that feeds the deep overflow contains components from both the Nordic Seas as well as deep waters from the Arctic Ocean, thus linking the Arctic to the global conveyor belt. Recent evidence suggests that water from the Arctic Ocean is becoming an increasingly important component of the deep water of the Nordic Sea as well as in the overflow water [e.g., *Karstensen et al.*, 2005; *Tanhua et al.*, 2005]. This provides a direct link between changing conditions in the Arctic Ocean and the World Ocean. In this paper we present measurements of the transient tracers chlorofluorocarbons (CFCs) and sulfur hexafluoride (SF_6) made in the Arctic Ocean during more that two decades. We use these data to calculate the ventilation of the Arctic Ocean, and we present estimates of the anthropogenic CO_2 (C_{ant}) content. The ventilation time of a water parcel is the time since it was last in contact with the atmosphere, where exchange of gases can take place. Depending on what assumptions are being made with regard to mixing, surface saturation, influence of bomb-derived ^{14}C, a range of ventilation times can be obtained from the same data. In this study we use the mean age of the transit time distribution, see below, as a measure of ventilation time.

[3] The volume of the central Arctic Ocean is close to 12.34×10^6 km^3. Together with several important shelf seas having a combined volume of about 0.65×10^6 km^3, the total volume is roughly 1% of the volume of the World Ocean [*Jakobsson*, 2002]. The Central Arctic Ocean is divided by ocean ridges into several sub-basins. The prominent Lomonosov Ridge divides the Arctic Ocean into the Eurasian and Canadian basins (the latter sometimes referred

[1]Marine Biogeochemistry, Leibniz Institute for Marine Sciences, Kiel, Germany.
[2]Bedford Institute of Oceanography, Dartmouth, Nova Scotia, Canada.
[3]Department of Chemistry, Gothenburg University, Göteborg, Sweden.
[4]Now at Bjerknes Center for Climate Research, Bergen, Norway.
[5]Lamont-Doherty Earth Observatory, Palisades, New York, USA.

0148-0227/09/2008JC004868$09.00

to as the Amerasian Basin, [*Björk et al.*, 2007]). The Eurasian Basin is divided into the Amundsen and the Nansen basins by the Gakkel Ridge, and the Canadian Basin is divided into the Canada and Makarov basins by the Alpha/Mendeleev Ridge. The shelves cover a proportionally significant area of the Arctic Ocean, comprising about 53% of the Arctic Ocean area, but contain only about 5% of its volume [*Jakobsson*, 2002].

1.1. Ventilation and Circulation of the Arctic Ocean

[4] The circulation of the intermediate water and the Atlantic Water is primarily along the topographic boundaries and the ocean ridge systems in the Arctic Ocean [e.g., *Rudels et al.*, 1994; *Jones et al.*, 1995]. Atlantic Water enters the Arctic through the Fram Strait and the Barents Sea. Important mixing and entrainment regions are located along the shelf, particularly east of the St. Anna Trough in the Kara Sea. The deep and intermediate layers of the Arctic Ocean are mainly ventilated via boundary convection processes that transport brine-enriched water formed over the shelf to the deep central basins as sinking plumes that descend the continental slope, entraining surrounding waters during the process [e.g., *Aagaard and Carmack*, 1989; *Wallace et al.*, 1992; *Rudels et al.*, 1994; *Jones et al.*, 1995; *Bönisch and Schlosser*, 1995; *Anderson et al.*, 1999; *Smethie et al.*, 2000]. The deep inflow through the Fram Strait of water originating in the Greenland Sea is an additional significant process of Arctic Ocean deep water ventilation [e.g., *Smethie et al.*, 1988; *Rudels et al.*, 2005]. Deep water is also exported from the Arctic Ocean through Fram Strait to the Greenland Sea and to the deeper part of the East Greenland Current [e.g., *Aagaard et al.*, 1991; *Rudels et al.*, 2005].

[5] There are only a handful of estimates of the ventilation time of the deep Arctic Ocean available in the literature. One reason is that the atmospheric time history for the CFCs is too short to capture the length residence times of the deep water [e.g., *Jones et al.*, 1995], with the exception of the most recent CFC data, as we shall see in this work. The CFC concentrations in the deep Eurasian Basin are typically close to, or below, the detection limit; whereas the CFC concentrations in the Canadian Basin are most often below the detection limit for the deep water [e.g., *Jones et al.*, 1995]. However, the related tracer carbon tetrachloride, CCl_4 has typically been found throughout the Arctic Ocean deep profiles [e.g., *Krysell and Wallace*, 1988; *Jones et al.*, 1995], indicating that CFCs should also be detected in the deep waters in the near future (CCl_4 has longer atmospheric history compared to the CFCs, making it a good tracer in slightly older water). Estimates of tracer ages from CFC and/or CCl_4 data have been incompatible with mean ages from isotope measurements, mainly because the different input functions and the unresolved issue of mixing in the "tracer age" calculations (generally simple comparison of the seawater concentrations to the corresponding atmospheric concentration for a specific time, see below).

[6] Even though the CFCs have been of somewhat limited value for old waters, estimates of mean ages, or ventilation times, of the Arctic Ocean deep waters have been calculated from isotope measurements. On the basis of a few ^{14}C profiles taken during the Oden cruise in 1991 in the Arctic Ocean, *Jones et al.* [1995] calculated the ventilation time of the Makarov Basin to be 360 years. Similarly, *Macdonald et al.* [1993] used ^{14}C from the Makarov Basin sampled during 1989 to calculate an effective deep water age of about 500 years. Further more, ^{39}Ar and ^{14}C data suggest that the Eurasian Basin deep water is 250–300 years, whereas the deep water in the Canadian Basin is approximately 450 years [*Schlosser et al.*, 1994, 1997]. Although this estimate is slightly lower than the 500–800 years ventilation time for the deep Canada Basin obtained by *Östlund et al.* [1987] based on ^{14}C profiles, it is reasonable to assume that the discrepancy can be explained by the somewhat higher uncertainties in the data set of *Östlund et al.* [1987]. Even though there is some uncertainty in these estimates due to scarcity of data and uncertainty in, for instance, the influence of bomb-^{14}C, there is certainly general agreement on the magnitude of the deep Arctic Ocean ventilation.

1.2. Arctic Ocean Anthropogenic CO_2 Inventory

[7] The storage of C_{ant} in the World Ocean is relatively high due to the buffering capacity of seawater; the ocean contains roughly 50 times more inorganic carbon than the atmosphere and is a significant sink of C_{ant} [*Canadell et al.*, 2007]. Good understanding and monitoring of the oceanic sink and uptake of C_{ant} is essential for our ability to understand and correctly assess the rapidly changing atmospheric, oceanic and terrestrial carbon reservoirs. However, because of scarcity of hydrochemical data in the Arctic Ocean, there are only a few estimates of the Arctic Ocean anthropogenic CO_2 inventory.

[8] Current observational based estimates of the global oceanic C_{ant} inventory for the year 1994 (excluding the Arctic Ocean and adjacent seas) range from 106 ± 17 petagrams of carbon (Pg = 10^{15} g) [*Sabine et al.*, 2004] to 94–121 Pg-C [*Waugh et al.*, 2006] using two very different techniques on the same data set (GLODAP [*Key et al.*, 2004]).

[9] Even though the Arctic Ocean volume contains only ~1% of the World Ocean volume [*Jakobsson*, 2002], it possibly contains as much as 5% of the global CFC-11 inventory [*Willey et al.*, 2004]. The Arctic Ocean has thus the potential to contribute significantly to the overall global C_{ant} inventory. A study based on data collected in 1991 calculated an Arctic Ocean inventory of 1.35 (1.29 to 1.47) Pg-C in 1991 [*Anderson et al.*, 1998b], corresponding to ~1.68 Pg-C in 2005, accounting only for the C_{ant} inventory below 500-m depth in the central basin. Since the Global Ocean stores half of its C_{ant} inventory above a depth of 400- to 500 m-depth [*Sabine et al.*, 2004; *Waugh et al.*, 2006], this approach underestimates the Arctic Ocean total C_{ant} inventory. In the ground breaking paper on the global C_{ant} inventory by *Sabine et al.* [2004], the Arctic Mediterranean Seas C_{ant} inventory was scaled to 5% of the global C_{ant} inventory. This estimate corresponds to ~4.9 Pg-C in the Arctic Ocean in 2005 (~6.4 Pg-C including the Nordic Seas). The scaling was based on the calculation of the global CFC-11 inventory from WOCE data [*Willey et al.*, 2004]. However, even if the presence of CFCs in the water column is an indicator for the presence of C_{ant}, the CFC inventory is an imperfect scaling factor for the C_{ant} inventory due to the differences in temperature and salinity dependency between C_{ant} and CFC. Whereas the CFC

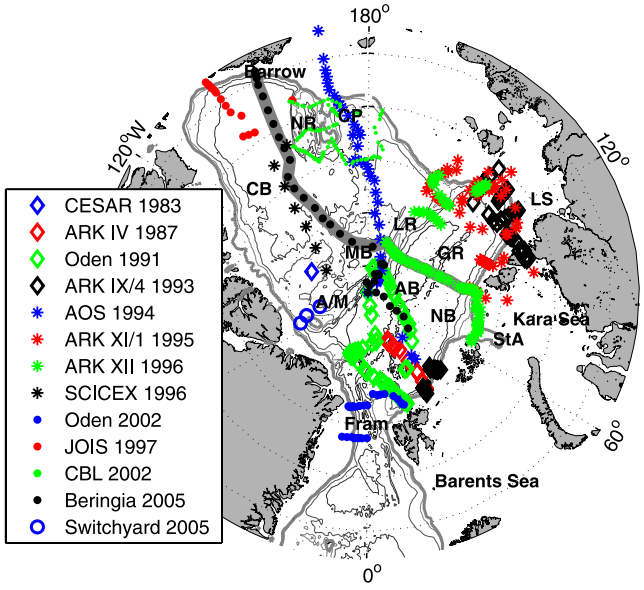

Figure 1. Map of the Arctic Ocean with stations for which CFC/SF_6 data are available (see Table 1). Some important basins and regions are marked on the map (MB, Makarov Basin; CB, Canada Basin, Barrow; CP, Chukchi Abyssal Plain; NR, Northwind Ridge; AB, Amundsen Basin; NB, Nansen Basin; and LS, Laptev Sea, Fram, Fram Strait; GR, Gakkel Ridge; LR, Lomonosov Ridge; A/M, Alpha/Mendeleev Ridge). The 500-m depth contour, marked with a thick gray line, together with the 80°N latitude in the Fram Strait, denotes the geographical boundary between the shelf and deep analyses, other depth contours every 1000 m [*Jakobsson et al.*, 2008]. The broad gray line shows the position of the section in Figure 4.

equilibrium concentration in seawater increases with decreasing temperature and salinity, the anthropogenic carbon equilibrium concentration behaves the opposite way due to the chemistry of the carbonate system in seawater [*Thomas and England*, 2002], which might be critical for the fresh and cold surface waters of the Arctic. Since the inventory estimate by *Sabine et al.* [2004] for the Arctic Ocean did not account for this effect, their calculation is likely an overestimate.

2. Methods and Data

2.1. Data Set

[10] In this study we have used the most comprehensive CFC and SF_6 transient tracer data set available for the Arctic Ocean, containing 535 hydrographic stations and 9723 individual tracer samples (Table 1 and Figure 1). The data span the period from the pioneering CESAR ice camp in 1983 [*Wallace and Moore*, 1985] to the Swedish/U.S. trans-arctic expedition Beringia in 2005. This data set provides an unmatched transient tracer database covering the Central Artic Ocean. However, the North American side of the Arctic Ocean is poorly sampled because of the generally heavy ice conditions, and there we are aware of only a few tracer profiles over the vast shelf areas.

2.2. Tracer Data

[11] For analytical precision and accuracies of the individual data sets we refer to the references in Table 1. The stated precisions are generally within WOCE standards. For this study, we used CFC-12 for most mean age and C_{ant} calculations since there is a positive atmospheric growth of CFC-12 through most of the sampling period, whereas CFC-11 concentration began to reverse in the early 1990s. For recently ventilated samples (i.e., pCFC-12 > 450ppt) we used measurements of SF_6, if available (i.e., part of the Beringia 2005 data), since SF_6 based C_{ant} (and mean age) estimates are less sensitive to errors in assumed saturation and measurements [*Tanhua et al.*, 2008]. For SCICEX96 we used CFC-11 data, since no CFC-12 data are available [*Smethie et al.*, 2000]. A critical property of the transient tracers is the saturation at the time of formation. Even though the Arctic Ocean is covered with sea ice during most of the year, the available CFC measurements show saturation levels that are comparable to open ocean values. For this analysis we have therefore adopted the time-dependent saturation of CFCs demonstrated by *Tanhua et al.* [2008], i.e., it is assumed that the saturation was 86% up to 1989 after which it increased linearly to 100% by year 1999, whereas the saturation of SF_6 is set at 85%.

Table 1. List of Tracer Data Sets (With Relevant References) Used in This Study[a]

Cruise	Ship	Year	CFC/SF_6 PI	Reference
CESAR	Ice Camp	1983	D.W.R. Wallace	*Wallace and Moore* [1985]
ARK IV	Polarstern	1987	D.W.R. Wallace	*Wallace et al.* [1992]
Oden91	Oden	1991	L.G. Anderson/E.P. Jones	*Anderson et al.* [1998a, 1999, 1994], *Rudels et al.* [1994]
Ark IX/4	Polarstern	1993	W.M. Smethie	*Frank et al.* [1998]
AOS94	Louis S. St-Laurent	1994	E.P. Jones	*Jones et al.* [1998], *Carmack et al.* [1997]
ARK XI/1	Polarstern	1995	W.M. Smethie	
ARK XII	Polarstern	1996	E.P. Jones	*Jones et al.* [1998], *Fransson et al.* [2001]
SCICEX 1996	USS Pogy	1996	W.M. Smethie	*Smethie et al.* [2000]
JOIS97	Louis S. St-Laurent	1997	E.P. Jones	*McLaughlin et al.* [2004]
Oden2002	Oden	2002	E.P. Jones	*Jeansson et al.* [2008], *Rudels et al.* [2005]
CBL2002	Polar Star	2002	W.M. Smethie	*Woodgate et al.* [2007, 2005]
Switchyard 2005	Airplane	2005	W.M. Smethie	*Smethie et al.* [2007]
Beringia	Oden	2005	L.G. Anderson	*Björk et al.* [2007]

[a]SF_6 data were only obtained from the Beringia 2005 cruise.

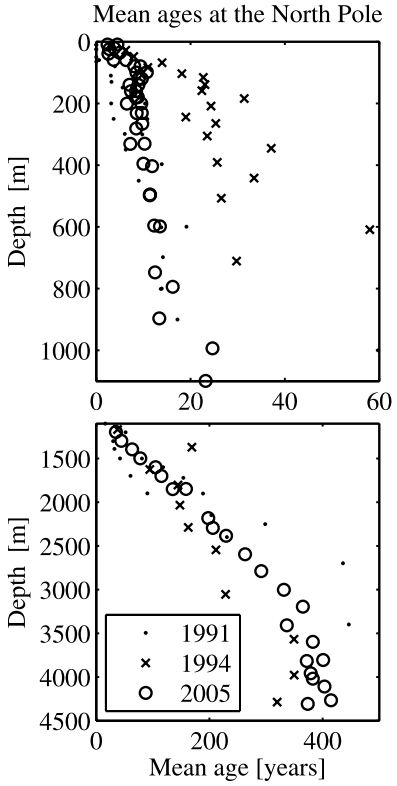

Figure 2. Mean ages (calculated with the TTD method) at the North Pole: 1991, 1994 and 2005.

2.3. TTD Method to Estimate C_{ant} Concentrations and Mean Ages

[12] The C_{ant} concentration has been calculated using the transit time distribution (TTD) method [*Hall et al.*, 2002; *Waugh et al.*, 2004, 2006]. The TTD method is based on measurements of transient tracers and a transfer function to scale the tracer concentrations to C_{ant}. With the TTD method, the C_{ant} concentration is a function of tracer content as well as carbonate chemistry, as we will show below.

[13] The concentration, c, of a passive tracer can be determined at any point, r, at any time, t, with knowledge of the TTD and the input function of the tracer at the sea surface, c_0 (t), according to;

$$c(r,t) = \int_0^\infty c_0(t-t')G(r,t')dt'$$

where G(r,t) is the TTD. The input function, c_0 (t), of the tracers at the sea surface is a function of the atmospheric history of the tracers and their solubilities. Here we have used the updated atmospheric history compilation by J. Bullister (available at http://cdiac.ornl.gov/oceans/new_atmCFC.html) for the CFCs and SF_6; for atmospheric CO_2 we have used updated records from Mauna Loa and Law Dome. The solubilities of the CFCs and SF_6 were calculated with the salinity and temperature relations provided by *Warner and Weiss* [1985] and *Bullister et al.* [2002], respectively. The transfer of inorganic carbon from the atmosphere to the ocean is further dependent on the buffer capacity (mainly a function of temperature and alkalinity) of seawater at the time when the water was last in contact with the atmosphere. It has been shown [*Jutterström and Anderson*, 2005] that the dissociation constants for the carbonate system from *Roy et al.* [1993] exhibit the best internal consistency for the Arctic Ocean. We therefore use those constants for the buffer capacity calculations together with the dissociation constants for boric acid from *Dickson* [1990]. We further use the surface salinity to alkalinity relation by *Brewer et al.* [1986] to determine the alkalinity of the water at the time of formation at the surface. Thus, with the knowledge of the atmospheric CO_2 concentration together with the temperature and salinity of the water, the equilibrium concentration of dissolved inorganic carbon (DIC) can be determined for each sample for any time, t, assuming that the salinity/alkalinity relation is valid also for the Arctic Ocean. The C_{ant} concentration for the surface water is then calculated as the difference between the DIC concentration at time t and the preindustrial concentration.

[14] The TTD of each interior location is assumed to be best represented by inverse Gaussian functions [*Waugh et al.*, 2003] in which the mixing is represented by two parameters; Γ, the mean age; and Δ, the width of the TTD. It should be pointed out that the mean age in the TTD calculation is different from the "tracer age" that is obtained by comparing the CFC concentration in seawater directly with the atmospheric history of CFCs. The TTD method implicitly includes mixing in the age calculations. Typically, the mean age is significantly higher than the "tracer age", and explains why there is such a large discrepancy between CFC ages and ages calculated with radioactive isotopes (i.e., ^{14}C).

[15] *Waugh et al.* [2004] demonstrated that the TTD of the ocean can be well approximated with $\Delta/\Gamma = 1$ using a combination of different tracers. With the assumption of a fixed relation between Γ and Δ, the TTD can be defined for each water sample by observation of a single transient tracer, such as CFC-12, CFC-11 or SF_6. Once the TTD is known, the concentration of any other tracer with a known input function, such as C_{ant}, can be determined. One way of testing the assumption of a fixed relation between Γ and Δ in the Arctic Ocean is to compare the mean ages at a station that has been repeated several times. Transient tracers will experience different input histories at different times, i.e., the seawater will have seen different parts of the atmospheric history. This is analogous to comparison of different tracers at the same point in time [e.g., *Waugh et al.*, 2003, 2004], with the difference that also changes in circulation/ventilation will influence the analysis. For this analysis we choose the North Pole, which has been sampled 3 times for CFCs in our data set, in 1991, 1994 and 2005. We calculated the mean age from these 3 repeats and compared the profiles (Figure 2). The upper water column (Figure 2, top) is fairly well ventilated, with mean ages less than 20 years. The exception is the data from1994, where significantly older water is present. This is a large change that can be explained neither by analytical/calibration errors nor by assuming any other Δ/Γ ratio, but is representing circulation changes, i.e., older water is dominating the halocline and Atlantic Water layers at the North Pole in 1994 compared to 1991 and 2005. This is confirmed by the very similar silicate concentrations at 400-m depth in 1991 and 2005 ($\sim$5 μmol

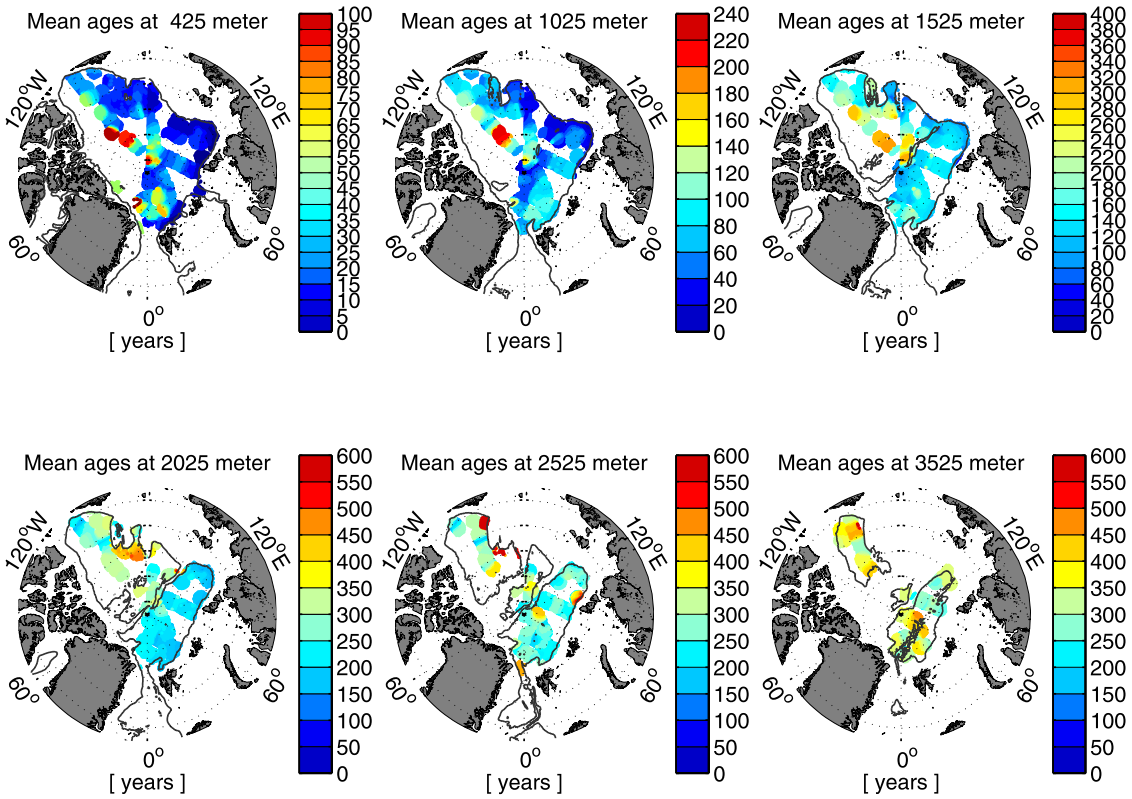

Figure 3. Mean ages for selected depth levels of the Arctic Ocean: 425, 1025, 1525, 2025, 2525 and 3525 m. Note that for this figure, the horizontal influence radius is set relatively short, that is, the mean ages are not extrapolated to cover the whole basin (see text section 2.3). Note different color scales of the figures. Depth contour is the bottom of the particular 50-m depth interval of each figure, using the topography from IBCAO v2.0 [*Jakobsson et al.*, 2008].

kg^{-1}), compared to the higher values in 1994 ($\sim$6.6 μmol kg^{-1}), indicating a shift of the front over the Lomonosov Ridge for the 1994 data, (Canada Basin Water is high in silicate at this depth [*Anderson et al.*, 1994; *Swift et al.*, 1997]). On the other hand, the 1991 and 2005 profiles are very similar to each other despite the two repeats being separated by 14 years, i.e., the two points in time will have experienced very different parts of the atmospheric history for CFC-12. If the $^{\Delta}/_{\Gamma}$ ratio was assumed to be different from one and if the circulation was constant, then the calculated mean ages would be different for the two repeats. Since we have seen that the assumption of steady state circulation at the North Pole does not seem to hold true, it could be a coincidence if the two profiles match each other, i.e., errors in the $^{\Delta}/_{\Gamma}$ ratio/analytical errors could cancel the effect of circulation changes. Another way of determining the $^{\Delta}/_{\Gamma}$ ratio is to compare two tracers with sufficiently different input functions, sampled at the same occasion (i.e., no interference from circulation changes). We used SF_6 and CFC-12 data from the Canada Basin for this comparison (similarly to the study by *Waugh et al.* [2004] and *Tanhua et al.* [2008], not shown), and the tracer distribution support the assumption of a $^{\Delta}/_{\Gamma}$ ratio equal to unity.

[16] In order to estimate C_{ant} concentrations based on tracer data from over two decades, and assuming the concept of transient steady state, we scale the C_{ant} concentrations to year 2005, the date of the most recent data set in our analysis. This concept states that for tracers with exponentially changing surface water concentrations, the vertical tracer profiles will reach "transient steady state" after a time period several times longer than the exponential growth timescale of the tracer. Once transient steady state is reached, the tracer depth profile will have a constant "shape", so that the tracer concentration at all depths changes proportionally to the surface concentration, i.e., if the change at the surface is known then the change at depth can be calculated [*Gammon et al.*, 1982; *Tanhua et al.*, 2007]. Since the atmospheric CO_2 concentrations in excess of 280 ppm can be regarded as the anthropogenic part, C_{ant} can be treated as a transient tracer with an exponentially increasing atmospheric history with an e-folding time of $\sim$70 years, i.e., the transient steady state concept is valid for C_{ant}. In practice, this means that, for instance, the C_{ant} concentrations calculated for the 1994 cruise with the TTD method has been multiplied with 1.20 to be comparable to the 2005 values. In a similar manner, it is possible to scale the C_{ant} inventories from previous studies to year 2005 in order to compare the results.

2.4. Mapping of the Data

[17] The profiles of mean ages and C_{ant} concentrations of the central Arctic Ocean were interpolated to 50-m intervals using piecewise cubic Hermite interpolation in a manner that does not allow extrapolation or interpolation over large depth intervals (depth-dependent). The interpolated profiles

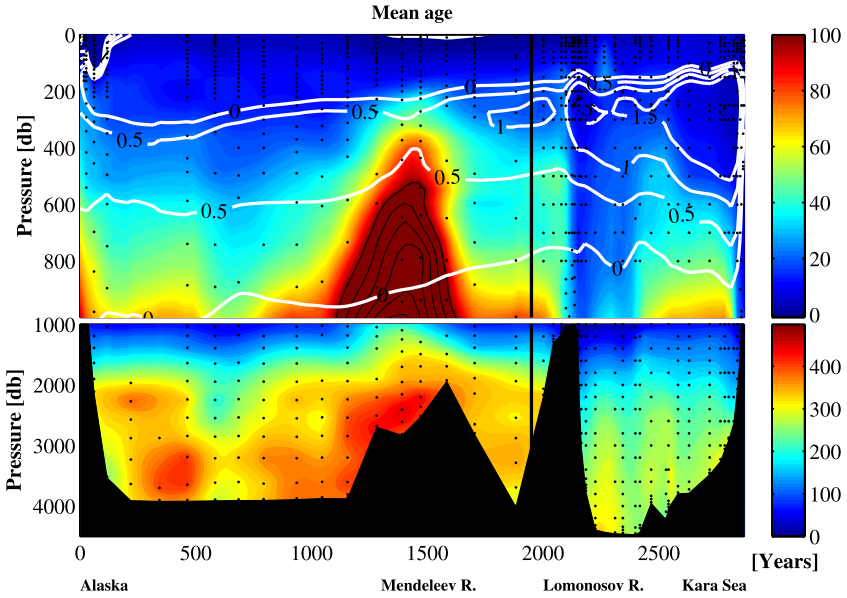

Figure 4. Section of mean age along the combined cruise tracks of the ARKXII cruise in 1996 and the Beringia 2005 cruise, see Figure 1 for location. The colors represent the mean age calculated with the TTD method. Note the different color scales for the two panels. The white contour lines are isotherms; the Atlantic Water layer has temperatures above 0°C (upper panel only). The black vertical line shows the boundary between the two cruises.

were then horizontally integrated on 50-m depth intervals in the central Arctic Ocean (defined as areas with depth >500 m, shallower areas are treated as the shelf, see below) using a mapping scheme where the distribution is controlled by topography and is influence by contours of barotropic potential vorticity f/H, where f is the planetary vorticity and H is the scaled water depth [*Rhein et al.*, 2002]. For the maps of C_{ant} we used a larger horizontal influence radius than for the mean age maps because of the need for a complete coverage of C_{ant} for the inventory calculation (horizontal scaling factors were 2×10^{-4} and 5×10^{-6} for mean age and C_{ant} maps, respectively, and the vertical scaling factor was 100 in both cases [*Rhein et al.*, 2002]). The interpolation errors are thus larger for the C_{ant} horizontal distributions than for the mean age distributions.

3. Results and Discussion

3.1. Ventilation and Mean Ages of the Arctic Ocean

[18] The mean age distributions for six selected depth layers in the Arctic Ocean are presented in Figure 3 (note the different color scales for the panels). In Figure 4, we present a section across the Arctic Ocean along the combination of the cruise tracks of the Beringia 2005 and the ARKXII in 1996 cruises (for map, see Figure 1). Regionally averaged profiles of the mean age are presented in Figure 5.

[19] During the most recent survey included in this study, the Beringia 2005, CFCs (and thus C_{ant}) were found in the deep layers of all major basins, putting an upper limit to the ventilation timescale of the deep Arctic Ocean to between 500 and 600 years. Note that mean ages of this magnitude correspond to CFC concentrations close to the analytical detection limit, and have therefore large uncertainty. The mean ages of the bottom waters are represented by the 3525-m distribution in Figure 3. The large scatter is partly representing the uncertainties in the transient tracer analysis at these concentration levels, but real distributions can be seen. There is a tendency to have somewhat more recently ventilated waters in the eastern part of the Eurasian Basin, where deep water formation is known to occur. More recently ventilated waters in the Canada Basin are also found close to the Chukchi Shelf, see below.

[20] The deep waters, above the bottom water, but still below the sill depth of the Lomonosov Ridge (1870 m [*Björk et al.*, 2007]) are represented by the distributions on 2525- and 2025-m depths. For these layers there are considerable mean age differences between the Eurasian and Canadian Basins, the Canadian Basin deep water is generally about 100 years older than the Eurasian Basin deep water. Significant horizontal age gradients are evident in the Canada Basin deep water, with better ventilated waters in the southern part of the basin. It appears that this water is formed locally in the southern Canada Basin since there is no evidence of transport of deep water from the Eurasian Basin/Fram Strait to this region [*Björk et al.*, 2007]. Formation of deep water in coastal polynyas over the Chukchi Shelf has been reported previously from observations and models [e.g., *Weingartner et al.*, 1998; *Winsor and Chapman*, 2002], and sinking plumes of dense water has been proposed to explain water mass properties in the Canada Basin [e.g., *Rudels et al.*, 1994; *Jones et al.*, 1995]. The data presented here suggest that locally formed deep water possibly can reach to the bottom of the basin, at least north of Barrow and east of Northwind Ridge. Particularly old waters are found north of Chukchi Abyssal Plain.

[21] Also, the ventilation of the intermediate depth waters (upper Polar Deep Water [*Rudels et al.*, 1999] range, here represented by the 1525 mean age distribution) show considerable spatial variations, particularly in the Canadian

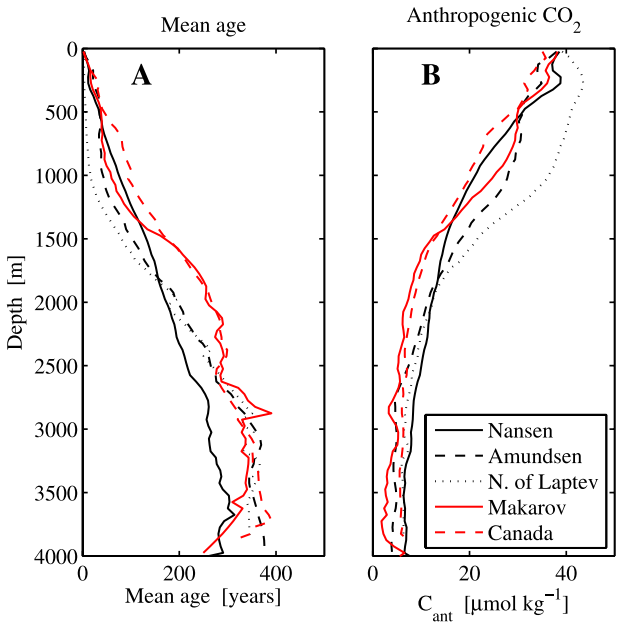

Figure 5. Regionally averaged profiles of (a) mean age (years) and (b) C_{ant} (μmol kg^{-1}), normalized to year 2005, for the central Arctic Ocean (excluding the shelf). Data from all cruises are used for these averages. Note that the region "N. of Laptev" refer to the area north of the shallow Laptev Sea.

Basin where the area around the Alpha/Mendeleev Ridge is "older". On the contrary, the Eurasian Basin north of the Laptev Sea seems to be particularly well ventilated, which confirms the presence of active boundary convection processes in this region. There is a sharp front across the Lomonosov Ridge, with significantly older water in the Makarov Basin. This is true for all depth levels below the Polar Mixed Layer, see Figure 4. The intense sampling of tracers around the Lomonosov Ridge at ~160°E in 2005 does not support any flow of Canadian Basin Deep Water to the Amundsen Basin as previously suggested [*Rudels et al.*, 1994; *Jones et al.*, 1995], and thus agrees with the results based on salinity and temperature from *Björk et al.* [2007]. The CFC data from the Beringia 2005 cruise also indicates a flow of Amundsen Basin water (higher CFC concentrations) on the Makarov side of the Lomonosov Ridge above 1500-m depth.

[22] We have chosen the 1025 m layer to represent the Barents Sea branch of the Atlantic layer. As discussed above, the Atlantic layer circulates in a mainly cyclonal manner around the Arctic, with several recirculation loops (e.g., Figure 9 in the study of *Rudels et al.* [1994]). The low ages along the Siberian shelf in the Eurasian Basin confirm the formation of this water type in this region (i.e., entering through the St. Anna Trough, [e.g., *Rudels et al.*, 1994]). At this depth level, the Amundsen Basin is considerably more recently ventilated than the Nansen Basin (except close to the shelf) (Figures 3 and 4). These observations indicate that there is a return flow of the Barents Sea branch along the Lomonosov Ridge in the Amundsen Basin. Again, the water over the southern slope of the Alpha/Mendeleev Ridge is "older" than the surrounding waters at the same depth layer.

[23] The ventilation of the Atlantic layer, Fram Strait branch, is represented by the 425 m mean age distribution. The main features of the circulation of the Atlantic Layer are clearly seen in Figure 3, where recently ventilated waters are found along the Eurasian shelf that include the inflow through Fram Strait and the St. Anna Trough. The high ages in the Nansen Basin are confined to the interior western part of the basin, possibly indicating contribution of older Atlantic Water that has already completed one loop around the Arctic Ocean. Recently ventilated water in the Amundsen Basin along the Lomonosov Ridge is clearly seen in Figure 3, confirming the short loop of the Atlantic Water in the Arctic Ocean. There is a sharp front in the mean ages over the Lomonosov Ridge, and somewhat more recently ventilated (and warmer) Atlantic Water in the southern part of the Makarov Basin. This is suggestive of a circulation loop of Atlantic Water in the Makarov Basin; see Figure 9 in the study of *Rudels et al.* [1994]. However, very high ventilation ages were observed over the southern flank of the Alpha/Mendeleev Ridge (Figure 4) during the Beringia 2005 cruise and during the SCICEX cruise in 1996 [*Smethie et al.*, 2000], which does not support a recirculation cell in the Canada Basin, at least not at the position where it is indicated by *Rudels et al.* [1994]. Note also that the high ages for station CESAR over the Alpha Ridge are not indicated in the map in Figure 3 since the mean age is in the order of 200 years, i.e., out of the scale of the plot. The circulation of intermediate water in the Canada Basin is discussed in detail by *Smethie et al.* [2000], and their conclusions are supported by the results presented here.

3.2. Distribution of Anthropogenic CO_2

[24] The distribution of C_{ant} closely resembles the inverse of the mean ages, see above. Figure 6 shows the C_{ant} concentration at the same 6 depth layers as in Figure 3. The highest concentrations are found along the borders of the Arctic Ocean, particularly north of the European shelf, just as expected from the circulation of the Atlantic layer. Since CFCs are present throughout the water column, anthropogenic carbon is also present throughout the water column. The bottom waters of the Arctic Ocean have a C_{ant} concentration of less than 8 μmol kg^{-1}, although with large relative uncertainties due to tracer concentrations being close to the detection limit. For the deep waters (represented by the 2525 and 2025 m water depths) there is considerably more C_{ant} in the Eurasian Basin than in the Canadian Basin, reflecting the mean age differences and also the influence of differences in temperature and salinity. Although warm and salty water tends to hold less CO_2 due to the solubility effects, this water can hold higher amounts of anthropogenic CO_2, due to the changes in the buffer factor [e.g., *Völker et al.*, 2002]. This is even more evident for the upper water levels that are influenced by the Atlantic Water, which is relatively saline and warm, and can thus carry a higher load of C_{ant}. The circulation of the Atlantic Water, and water influenced by the Atlantic layer along the Eurasian Shelf and along the Lomonosov Ridge, is clearly visible in Figure 6 (top). There are particularly low concentrations in the Canada/Makarov Basin and over the Alpha Ridge. The highest concentrations of C_{ant} are found in the upper

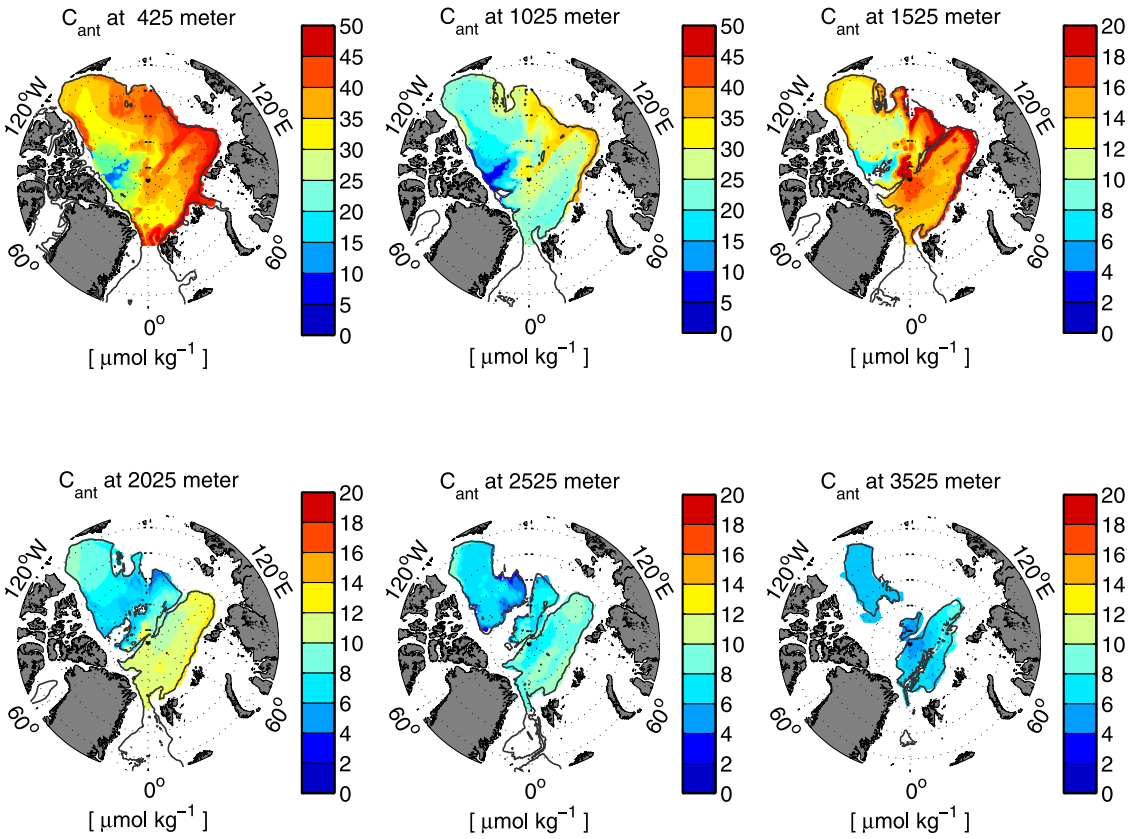

Figure 6. Anthropogenic CO_2 concentrations for selected depth levels of the Arctic Ocean: 425, 1025, 1525, 2025, 2525 and 3525 m. The C_{ant} concentrations are calculated with the TTD method from transient tracer data, assuming that the value of the mean age and the width are equal ($\Delta/\Gamma = 1$). Note different color scales of the figures. Depth contours are the bottom of the particular 50-m depth interval of each image.

layers of the Amundsen and Nansen basins, particularly in the area north of the Laptev Sea. The vertical distribution of C_{ant} is also illustrated by regionally averaged C_{ant} profiles (Figure 5). The C_{ant} concentrations near the 1000-m depth are lowest for the interior Nansen Basin and highest north of the Laptev Sea.

3.3. Central Arctic Ocean C_{ant} Inventory

[25] The C_{ant} inventory for each individual layer within the 500m depth contour (every 50 m) is calculated using the horizontal integration scheme discussed in section 2.3. The inventories of each layer are then added up to obtain the full C_{ant} inventory of the central Arctic Ocean. In this way, we calculate the Central Arctic Ocean C_{ant} inventory to be 2.73 Pg-C, normalized to year 2005.

[26] As discussed above, this estimate assumes that the air-sea disequilibrium of CO_2 has remained constant since the beginning of the industrialization. If the air-sea disequilibrium changes with time, then our C_{ant} estimate will be biased. For instance, in the global assessment of C_{ant} using the TTD method, *Waugh et al.* [2006] found that the TTD method may overestimate the C_{ant} inventory in the Southern Ocean by as much as 60% compared to a General Circulation Model. This is due to low "saturation" of C_{ant} in regions of deep convection, which leads to time-variant air-sea equilibration of CO_2 in the model. However, because of the shorter timescale for air-sea equilibration of CFCs than for CO_2, the saturation of the CFCs was not significantly different from other high latitude oceans in the model. This results in an overestimation of the C_{ant} concentrations by this application of the TTD method.

[27] How might this potentially biasing change in air-sea disequilibrium over time affect our C_{ant} inventory estimate of the Arctic Ocean? Approximately the top 1000 m of the water column in the Arctic Ocean is dominated by either the Atlantic Water or the fresher and locally ventilated Polar Mixed layer [*Rudels et al.*, 1999], only the deeper layers are formed convectively within the Arctic Ocean, see section 1.1. Furthermore, the entrainment of well ventilated Atlantic Water is important for the convective processes in the Arctic Ocean, which adds to the differences in deep water formation between the Arctic and the Southern Ocean [*Anderson et al.*, 1999]. In our analysis, we find 1.06 Pg-C of C_{ant} below the influence of the Atlantic layer (i.e., below 1000 m) in the Central Arctic Ocean. If the TTD method over estimates the C_{ant} concentrations in the deep layers of the Arctic Ocean by 25–50% due to time-variant air-sea equilibrium of CO_2, similarly to the situation in the Southern Ocean, then the Arctic Ocean C_{ant} inventory would be reduced by 0.40 ± 0.13 Pg-C. However, *Waugh et al.* [2006] found excellent agreement with the TTD derived C_{ant} inventories and the inventories from the model in all regions except the

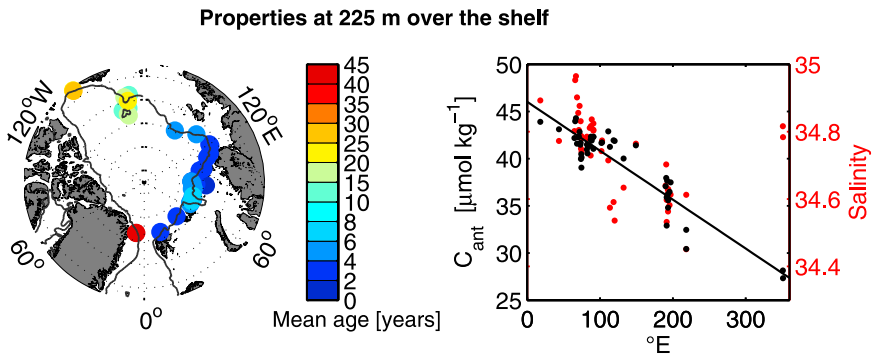

Figure 7. Properties at 225 m for the 47 stations over the shelf break in our data set. (left) A map with the mean age at 225 m in color coding (note the nonlinear color coding). (right) C_{ant} concentrations (black dots) and salinities (red dots) at 225 m plotted as a function of longitude (0°–360°E), the linear fit is for C_{ant} data.

Southern Ocean. It is therefore uncertain if this correction should be applied to the Arctic Ocean; rather it defines the upper limit of the uncertainty in the inventory calculations.

3.4. Arctic Ocean Shelf C_{ant} Inventory

[28] Our primary analysis is focused on the central Arctic Ocean basin as there are relatively few tracer data from the shelf regions. However, since the highest concentrations of C_{ant} are generally found in the well ventilated surface layers, we will attempt to estimate the C_{ant} inventory for the shelf and adjacent seas as well. In addition to direct ventilation to the atmosphere, the shallow layers are influenced by well ventilated Atlantic Water (AW) high in salinity, temperature and, consequently, anthropogenic carbon. This water mass circulates the Arctic Ocean primarily in a cyclonic manner, and is thus less recently ventilated when it exits the Arctic Ocean as modified Atlantic Water [*Jones et al.*, 1995; *Frank et al.*, 1998; *Rudels et al.*, 1999]. One would thus expect to find decreasing concentrations of C_{ant}, increasing mean ages and decreasing salinities (due to dilution of the AW with low salinity shelf water and Pacific Water [e.g., *Jones et al.*, 2008]) along the path of the main circulation. This is indeed what we find at the 225-m depth for the 47 shelf stations in our data set (Figure 7). The mean age is generally increasing along the circulation pathway (Figure 7, left) with recently ventilated waters entering the Arctic through Fram Strait and over the Barents Sea/Kara Sea. Figure 7 (right) shows that the salinity is decreasing along the circulation (except for the stations west of Fram Strait where AW recirculated within the Arctic seems to increase the salinity), and that the C_{ant} concentration is nearly linearly decreasing vs. longitude. The decreasing C_{ant} concentrations along the circulation are thus the combined effect of freshening and aging of this layer (less salty water hold less C_{ant}, as do less recently ventilated waters).

[29] We extrapolated the C_{ant} concentrations for each shelf area by using available tracer measurements, the C_{ant} vs. longitude relationship in Figure 7, and the volumetric data for the "shelf seas" from *Jakobsson* [2002]. On the basis of this we estimate the C_{ant} inventory to 0.30 Pg-C over the Arctic Ocean shelf (normalized to year 2005). Approximately 10% of the total Arctic Ocean C_{ant} inventory (and ~0.25% of the global oceanic C_{ant} inventory) is thus stored over the Arctic Ocean shelf. A caveat in these calculations is the influence of low salinity (e.g., low alkalinity) river waters in the nearshore areas that have lower capacity to store C_{ant}. Our C_{ant} estimate for the shelf is therefore an upper limit, even though the nearshore, low alkalinity areas, are generally shallow, i.e., have a small volume.

3.5. CFC-11 Inventory

[30] The CFC-11 inventory of the Arctic Ocean has been calculated to be 28×10^6 moles, which is 5% of the global oceanic inventory of 550×10^6 moles based mainly on the WOCE data set [*Willey et al.*, 2004]. Since the data set used in this study is much more comprehensive for the Arctic Ocean, we provide an updated CFC-11 inventory estimate.

[31] The atmospheric CFC-11 concentration increased until the early 1990s, after which it has been decreasing. It is thus difficult to directly compare CFC-11 measurements sampled over more than 2 decades, and to calculate the inventory from these data. However, with knowledge of the TTD, the concentration of any other passive tracer can be calculated for any time, as described in section 2.3. Since we have already calculated the TTD field of the Arctic Ocean from CFC-12 and SF_6 data, we use this information to calculate the CFC inventory in a way similar to how the C_{ant} inventory was calculated.

[32] We find that the central Arctic Ocean CFC-11 inventory was 22.1×10^6 moles in 1994 and 29.5×10^6 moles in 2005. Interestingly, the inventory over the shelf did not change during this time frame, but remains at 4.1×10^6 moles. This is an effect of decreasing surface concentrations being balanced by increasing concentrations at depth (i.e., for somewhat older water where the concentrations are still increasing).

3.6. Uncertainties

[33] Uncertainties in estimating C_{ant} with the TTD method from CFC-12 and SF_6 data have recently been calculated by *Tanhua et al.* [2008]. We used these calculations to address the uncertainties due to analytical errors and errors in correctly assessing the saturation of the tracers. We find that uncertainty in the inventory is ±0.21 Pg-C (i.e., ±7%) for the Arctic Ocean. This estimate includes aspects such as large uncertainties for recently sampled and recently ventilated waters (due to the small (or reversed) atmospheric

growth rate of the CFCs), as well as over estimation of the C_{ant} concentration in low CFC waters due to instrumental and sampling blanks in the measurements. We estimate that the random error due to mapping uncertainties is ±5% (±0.15 Pg-C). The uncertainty associated with the Δ/Γ ratio for the C_{ant} calculation is of the order of 1 μmol kg^{-1} [*Waugh et al.*, 2004], i.e. ±0.16 Pg-C for the whole Arctic Ocean. The total uncertainty due to analytical, C_{ant} calculation and mapping uncertainties is thus ±0.30 Pg-C. Adding to this the uncertainty of 0.4 Pg-C derived from time-variant air-sea disequilibrium, as discussed above, and assuming that this error can only bias the TTD derived estimate to be too high (i.e., assuming that the CO_2 air-sea equilibrium could have increased over time, but not decreased). This means that the range of uncertainties is −0.5 to +0.3 Pg-C for the Arctic Ocean C_{ant} inventory. The uncertainties in the CFC-11 inventory calculations are related to those of the C_{ant} calculations (except that the air-sea equilibrium changes for CO_2 do not apply to the CFC-11 calculations), i.e., ±10%.

4. Summary and Conclusions

[34] The mean ages of the upper water column supports the general circulation along the topographic boundaries and ridge systems except over the Alpha/Mendeleev Ridge, where water with high age is found. The ventilation time for the intermediate water column is shorter in the Eurasian Basin (∼200 y) than in the Canadian Basin (∼300 y) where the deep and bottom waters have CFC values which are close to the detection limit and lower than in the Eurasian Basin.

[35] Our best estimate of the C_{ant} inventory, normalized to year 2005, is thus 3.0 Pg-C (2.7 Pg-C for the Central Arctic Ocean and 0.30 Pg-C for the shelf areas). Including the uncertainties discussed above, the inventory range is 2.5–3.3 Pg-C for the Arctic Ocean (central Arctic Ocean and the shelf). This is a significant number in the global budget for anthropogenic carbon that can now, with some confidence, be added to the oceanic C_{ant} reservoir (the global C_{ant} inventory is 118 ± 19 Pg-C or 142 ± 23 Pg-C if normalized to year 2005, according to *Sabine et al.* [2004]). Our estimate is ∼1.9 Pg-C lower than the rough estimate of ∼4.9 Pg-C by *Sabine et al.* [2004] for the Arctic Ocean. We find that approximately 1.8 Pg-C, i.e., ∼52% of the total Arctic Ocean C_{ant} inventory, is found deeper than 500 m, which is within the uncertainties of the estimates of 1.68 Pg-C by *Anderson et al.* [1998b]. We further calculate the Arctic Ocean CFC-11 inventory to be 26.2 ± 2.6 × 10^6 moles for year 1994, which is comparable with the Arctic Ocean inventory of 28 × 10^6 moles reported by *Willey et al.* [2004].

[36] Our estimates thus suggest that the Arctic Ocean stores ∼2% of the global oceanic C_{ant} inventory but as much as ∼ 5% of the global oceanic CFC-11 inventory, despite compromising only 1% of the global ocean volume. The difference between the C_{ant} and CFC-11 inventories can be explained by the opposing effects of temperature and salinity (also alkalinity for C_{ant}, which is correlated to the salinity) on the carbonate chemistry and gas solubility for C_{ant} and CFC-11, respectively. For instance, the equilibrium concentration of CFC-11 is roughly twice as high in water with salinity 32 and temperature −1.7°C (i.e., Arctic surface water), as in "typical" mid-latitude surface water (salinity 35 and temperature 10°C), whereas the C_{ant} equilibrium concentration for the Arctic water is only about 70% of the midlatitude water.

[37] **Acknowledgments.** We thank all persons involved in the measurement of the tracer and hydrographic data used in this synthesis, not only the science party but also the crew and captains of the numerous icebreakers that have been pushing through the Arctic ice. The manuscript benefited from financial support from the Swedish Polar Research Secretariat, the Swedish Research Council, the EU projects CarboOcean (Project 511176) and DAMOCLES (Project 018509), Canada Panel on Energy Research and Development (EPJ), and United States NSF OPP01-17367 and OPP02-30238.

References

Aagaard, K., and E. C. Carmack (1989), The role of sea ice and fresh water in the Arctic circulation, *J. Geophys. Res.*, *94*, 14,485–14,498.

Aagaard, K., E. Fahrbach, J. Meincke, and J. H. Swift (1991), Saline outflow from the Arctic Ocean: Its contribution to the deep waters of the Greenland, Norwegian, and Iceland seas, *J. Geophys. Res.*, *96*, 20,433–20,441.

Anderson, L. G., G. Björk, O. Holby, E. P. Jones, G. Kattner, K. P. Koltermann, B. Liljeblad, R. Lindegren, B. Rudels, and J. Swift (1994), Water masses and circulation in the Eurasian Basin—Results from the Oden 91 Expedition, *J. Geophys. Res.*, *99*, 3273–3283.

Anderson, L. G., K. Olsson, and M. Chierici (1998a), A carbon budget for the Arctic Ocean, *Global Biogeochem. Cycles*, *12*, 455–465.

Anderson, L. G., K. Olsson, E. P. Jones, M. Chierici, and A. Fransson (1998b), Anthropogenic carbon dioxide in the Arctic Ocean: Inventory and sinks, *J. Geophys. Res.*, *103*, 27,707–27,716.

Anderson, L. G., E. P. Jones, and B. Rudels (1999), Ventilation of the Arctic Ocean estimated by a plume entrainment model constrained by CFCs, *J. Geophys. Res.*, *104*, 13,423–13,429.

Björk, G., et al. (2007), Bathymetry and deep-water exchange across the central Lomonosov Ridge at 88–89 degrees N, *Deep Sea Res., Part I*, *54*, 1197–1208, doi:10.1016/j.dsr.2007.05.010.

Bönisch, G., and P. Schlosser (1995), Deep water formation and exchange rates in the Greenland/Norwegian seas and the Eurasian Basin of the Arctic Ocean derived from tracer balances, *Prog. Oceanogr.*, *35*, 29–52.

Brewer, P., A. L. Bradshaw, and R. T. Williams (1986), Measurements of total carbon dioxide and alkalinity in the North Atlantic Ocean in 1981, in *The Changing Carbon Cycle: A Global Analysis*, edited by J. R. Trabalka and D. E. Reichele, 348–370, Springer-Verlag, New York.

Bullister, J. L., D. P. Wisegarver, and F. A. Menzia (2002), The solubility of sulfur hexafluoride in water and seawater, *Deep Sea Res., Part I*, *49*, 175–187.

Canadell, J. G., C. Le Quéré, M. R. Raupach, C. B. Field, E. Buitenhuis, P. Ciais, T. J. Conway, N. P. Gillett, R. A. Houghton, and G. Marland (2007), Contributions to accelerating atmospheric CO_2 growth from economic activity, carbon intensity, and efficiency of natural sinks., *Proc. Natl. Acad. Sci. U. S. A.*, *104*, 18,866–18,870.

Carmack, E. C., K. Aagaard, J. H. Swift, R. W. MacDonald, F. A. McLaughlin, E. P. Jones, R. G. Perkin, J. N. Smith, K. M. Ellis, and L. R. Killius (1997), Changes in temperature and tracer distributions within the Arctic Ocean: Results from the 1994 Arctic Ocean section, *Deep Sea Res., Part II*, *44*, 1487–1502.

Dickson, G. D. (1990), Thermodynamics of the dissociation of boric acid in synthetic seawater from 273.15 to 318.15 K., *Deep Sea Res.*, *37*, 755–766.

Frank, M., W. M. Smethie, and R. Bayer (1998), Investigation of subsurface water flow along the continental margin of the Eurasian Basin using the transient tracers tritium, He-3, and CFCs, *J. Geophys. Res.*, *103*, 30,773–30,792.

Fransson, A., M. Chierici, L. G. Anderson, I. Bussmann, G. Kattner, E. P. Jones, and J. H. Swift (2001), The importance of shelf processes for the modification of chemical constituents in the waters of the Eurasian Arctic Ocean: Implication for carbon fluxes, *Cont. Shelf. Res.*, *21*, 225–242.

Gammon, R. H., J. Cline, and D. P. Wisegarver (1982), Chlorofluoromethanes in the Northeast Pacific Ocean: Measured vertical distribution and application as transient tracers of upper ocean mixing, *J. Geophys. Res.*, *87*, 9441–9454.

Hall, T. M., T. N. Haine, and D. W. Waugh (2002), Inferring the concentration of anthropogenic carbon in ocean from tracers, *Global Biogeochem. Cycles*, *16*(4), 1131, doi:10.1029/2001GB001835.

Jakobsson, M. (2002), Hypsometry and volume of the Arctic Ocean and its constituent seas, *Geochem. Geophys. Geosyst.*, *3*(5), 1028, doi:10.1029/2001GC000302.

Jakobsson, M., R. Macnab, L. Mayer, R. Anderson, M. Edwards, J. Hatzky, H. W. Schenke, and P. Johnson (2008), An improved bathymetric portrayal of the Arctic Ocean: Implications for ocean modeling and geological, geophysical and oceanographic analyses, *Geophys. Res. Lett.*, *35*, L07602, doi:10.1029/2008GL033520.

Jeansson, E., S. Jutterström, B. Rudels, L. G. Anderson, K. A. Olsson, E. P. Jones, W. M. Smethie Jr., and J. H. Swift (2008), Sources to the East Greenland Current and its contribution to the Denmark Strait overflow, *Prog. Oceanogr.*, *78*, 12–28, doi:10.1016/j.pocean.2007.08.031.

Jones, E. P., B. Rudels, and L. G. Anderson (1995), Deep waters of the Arctic Ocean: Origins and circulation, *Deep Sea Res., Part I*, *42*, 737–760.

Jones, E. P., L. G. Anderson, and J. H. Swift (1998), Distribution of Atlantic and Pacific waters in the upper Arctic Ocean: Implications for circulation, *Geophys. Res. Lett.*, *25*, 765–768.

Jutterström, S., and L. G. Anderson (2005), The saturation of calcite and aragonite in the Arctic Ocean, *Mar. Chem.*, *94*, 101–110, doi:10.1016/j.marchem.2004.08.010.

Karstensen, J., P. Schlosser, D. W. R. Wallace, J. L. Bullister, and J. Blindheim (2005), Water mass transformation in the Greenland Sea during the 1990s, *J. Geophys. Res.*, *110*, C07602, doi:10.1029/2004JC002510.

Key, R. M., A. Kozyr, C. L. Sabine, K. Lee, R. Wanninkhof, J. L. Bullister, R. A. Feely, F. J. Millero, C. Mordy, and T. H. Peng (2004), A global ocean carbon climatology: Results from Global Data Analysis Project (GLODAP), *Global Biogeochem. Cycles*, *18*, GB4031, doi:10.1029/2004GB002247.

Krysell, M., and D. W. R. Wallace (1988), Arctic Ocean ventilation studied with a suite of anthropogenic halocarbon tracers, *Science*, *242*, 746–749.

Macdonald, R. W., E. C. Carmack, and D. W. R. Wallace (1993), Tritium and radiocarbon dating of Canada Basin deep waters, *Science*, *259*, 103–104.

McLaughlin, F. A., E. C. Carmack, R. W. Macdonald, H. Melling, J. H. Swift, P. A. Wheeler, B. F. Sherr, and E. B. Sherr (2004), The joint roles of Pacific and Atlantic-origin waters in the Canada Basin, 1997–1998, *Deep Sea Res., Part I*, *51*, 107–128.

Östlund, G., G. Possnert, and J. Swift (1987), Ventilation rate of the deep Arctic Ocean from carbon-14 data, *J. Geophys. Res.*, *92*, 3769–3777.

Rhein, M., J. Fischer, W. M. Smethie, D. Smythe-Wright, R. F. Weiss, C. Mertens, D. H. Min, U. Fleischmann, and A. Putzka (2002), Labrador seawater: Pathways, CFC inventory, and formation rates, *J. Phys. Oceanogr.*, *32*, 648–665.

Roy, R. N., L. N. Roy, K. N. Vogel, C. Porter-Moore, T. Pearson, C. E. Good, F. J. Millero, and D. M. Campbell (1993), The dissociation constants of carbonic acid in seawater at salinities 5 to 45 and temperatures 0 to 46 deg C., *Mar. Chem.*, *44*, 249–267.

Rudels, B., E. P. Jones, L. G. Anderson, and G. Kattner (1994), On the intermediate depth waters of the Arctic Ocean, in *The Polar Oceans and Their Role in Shaping the Global Environment*, edited by R. Muench and O. M. Johannesson, pp. 33–46, AGU, Washington, D. C.

Rudels, B., H. J. Friedrich, and D. Quadfasel (1999), The Arctic circumpolar boundary current, *Deep Sea Res., Part II*, *46*, 1023–1062.

Rudels, B., G. Björk, J. Nilsson, P. Winsor, I. Lake, and C. Nohr (2005), The interaction between waters from the Arctic Ocean and the Nordic Seas north of Fram Strait and along the East Greenland Current: Results from the Arctic Ocean-02 Oden expedition, *J. Mar. Syst.*, *55*, 1–30, doi:10.1016/j.marsys.2004.06.008.

Sabine, C. L., et al. (2004), The oceanic sink for anthropogenic CO_2, *Science*, *305*, 367–371.

Schlosser, P., B. Kromer, G. Östlund, B. Ekwurzel, G. Bönisch, H. H. Loosli, and R. Purtschert (1994), On the 14-C and 39-Ar distribution in the central Arctic Ocean: Implications for the deep water formation, *Radiocarbon*, *36*, 327–343.

Schlosser, P., B. Kromer, B. Ekwurzel, G. Bönisch, A. McNichol, R. Schneider, K. von Reden, H. G. Ostlund, and J. H. Swift (1997), The first trans-Arctic C-14 section: Comparison of the mean ages of the deep waters in the Eurasian and Canadian basins of the Arctic Ocean, *Nucl. Instrum. Methods Phys. Res., Sect. B*, *123*, 431–437.

Smethie, W. M., Jr., D. W. Chipman, J. H. Swift, and K. P. Koltermann (1988), Chlorofluoromethanes in the Arctic Mediterranean seas: Evidence for formation of bottom water in the Eurasian Basin and deep-water exchange through Fram Strait, *Deep Sea Res., Part A*, *35*, 347–369.

Smethie, W. M., Jr., P. Schlosser, G. Bönisch, and T. S. Hopkins (2000), Renewal and circulation of intermediate waters in the Canadian Basin observed on the SCICEX 96 cruise, *J. Geophys. Res.*, *105*, 1105–1121.

Smethie, W. M., P. Schlosser, B. Newton, M. Steele, and J. Morison (2007), Composition of upper Arctic Ocean water masses north of Ellesmere Island, *Eos Trans. AGU*, *88*(52), Fall Meet. Suppl., Abstract U41C-0621.

Swift, J. H., E. P. Jones, K. Aagaard, E. C. Carmack, M. Hingston, R. W. Macdonald, F. A. McLaughlin, and R. G. Perkins (1997), Waters of the Makarov and Canada Basins, *Deep Sea Res., Part II*, *44*(8), 1503–1529.

Tanhua, T., K. A. Olsson, and E. Jeansson (2005), Formation of Denmark Strait Overflow Water and its hydro-chemical composition, *J. Mar. Syst.*, *57*, 264–288, doi:10.1016/j.jmarsys.2005.05.003.

Tanhua, T., A. Körtzinger, K. Friis, D. W. Waugh, and D. W. R. Wallace (2007), An estimate of anthropogenic CO_2 inventory from decadal changes in ocean carbon content, *Proc. Natl. Acad. Sci. U. S. A.*, *104*, 3037–3042, doi:10.1073/pnas.0606574104.

Tanhua, T., D. W. Waugh, and D. W. R. Wallace (2008), Use of SF_6 to estimate anthropogenic carbon in the upper ocean, *J. Geophys. Res.*, *113*, C04037, doi:10.1029/2007JC004416.

Thomas, H., and M. England (2002), Different oceanic features of anthropogenic CO_2 and CFCs, *Naturwissenschaften*, *89*, 399–403.

Völker, C., D. W. R. Wallace, and D. A. Wolf-Gladrow (2002), On the role of heat fluxes in the uptake of anthropogenic carbon in the North Atlantic, *Global Biogeochem. Cycles*, *16*(4), 1138, doi:10.1029/2002GB001897.

Wallace, D. W. R., and R. M. Moore (1985), Vertical profiles of CCl_3F (F-11) and CCl_2F_2 (F-12) in the central Arctic Ocean-Basin, *J. Geophys. Res.*, *90*, 1155–1166.

Wallace, D. W. R., P. Schlosser, M. Krysell, and G. Bönisch (1992), Halocarbon ratio and tritium/3He dating of water masses in the Nansen Basin, Arctic Ocean, *Deep Sea Res., Part I*, *39*, 435–458.

Warner, M. J., and R. F. Weiss (1985), Solubilities of chlorofluorocarbons 11 and 12 in water and sea water, *Deep Sea Res.*, *32*, 1485–1497.

Waugh, D. W., T. M. Hall, and T. W. N. Haine (2003), Relationship among tracer ages, *J. Geophys. Res.*, *108*(C5), 3138, doi:10.1029/2002JC001325.

Waugh, D. W., T. M. Hall, and T. W. N. Haine (2004), Transport times and anthropogenic carbon in the subpolar North Atlantic Ocean, *Deep Sea Res., Part I*, *51*, 1471–1491, doi:10.1016/j.dsr.2004.06.011.

Waugh, D. W., T. M. Hall, B. I. McNeil, R. Key, and R. J. Matear (2006), Anthropogenic CO_2 in the oceans estimated using transit-time distributions, *Tellus*, *58B*, 376–389, doi:10.1111/j.1600-0889.2006.00222.x.

Weingartner, T. J., D. J. Cavalieri, K. Aagaard, and Y. Sasaki (1998), Circulation, dense water formation, and outflow on the northeast Chukchi shelf, *J. Geophys. Res.*, *103*, 7647–7661.

Willey, D. A., R. A. Fine, R. E. Sonnerup, J. L. Bullister, W. M. Smethie Jr., and M. J. Warner (2004), Global oceanic chlorofluorocarbon inventory, *Geophys. Res. Lett.*, *31*, L01303, doi:10.1029/2003GL018816.

Winsor, P., and D. C. Chapman (2002), Distribution and interannual variability of dense water production from coastal polynyas on the Chukchi Shelf, *J. Geophys. Res.*, *107*(C7), 3079, doi:10.1029/2001JC000984.

Woodgate, R. A., K. Aagaard, J. H. Swift, K. K. Falkner, and W. M. Smethie Jr. (2005), Pacific ventilation of the Arctic Ocean's lower halocline by upwelling and diapycnal mixing over the continental margin, *Geophys. Res. Lett.*, *32*, L18609, doi:10.1029/2005GL023999.

Woodgate, R. A., K. Aagaard, J. H. Swift, W. M. Smethie Jr., and K. K. Falkner (2007), Atlantic water circulation over the Mendeleev Ridge and Chukchi Borderland from thermohaline intrusions and water mass properties, *J. Geophys. Res.*, *112*, C02005, doi:10.1029/2005JC003416.

L. G. Anderson and S. Jutterström, Department of Chemistry, Gothenburg University, SE-412 96 Göteborg, Sweden.

E. Jeansson, Bjerknes Center for Climate Research, Allegaten 55, 5007 Bergen, Norway.

E. P. Jones, Ocean Science Division, Bedford Institute of Oceanography, 1 Challenger Drive, P.O. Box 1006, Dartmouth, NS B2Y 4A2, Canada.

W. M. Smethie Jr., Lamont-Doherty Earth Observatory, 129 Comer, 61 Route, 9W-PO Box 1000, Palisades, NY, USA.

T. Tanhua and D. W. R. Wallace, Marine Biogeochemistry, Leibniz Institute for Marine Sciences, Kiel D-24105, Germany. (ttanhua@ifm-geomar.de)